*Original Paper* *Forma*, **15**, 377–391, 2000

# Analysis of Sliding Actin Filaments Utilizing a Novel Method of Spatiotemporal Color Patterns

Satoshi HASEGAWA[1,2] and Koshin MIHASHI[2]

[1]*School of Information Culture, Nagoya Bunri University, Inazawa, Aichi 492-8520, Japan*
[2]*Graduate School of Mathematics, Nagoya University, Chikusa-ku, Nagoya 464-8602, Japan*

(Received December 24, 1999; Accepted April 19, 2000)

**Keywords:** Image Processing, Computer Visualization, Pattern, Actin Filament, Motility Assay

**Abstract.** The study of sliding movements of actin filaments on a surface-fixed myosin in an *in vitro* motility assay presents a useful method employed to understand the mechanisms of muscle contraction. In order to gain insight into this study, we here propose a novel method to create "spatiotemporal color patterns" of a moving thin filament. First, we verified the method by using artificial patterns generated by computer simulations. Then we gleaned coordinate data of actin filaments from video images by applying digital processing, and expressed the results with the patterns. With this method, the existence of fluctuations in the sliding velocity and/or locus were clearly visualized. As a result, we could also develop a new effective method to accurately determine the sliding velocity of the transforming filaments. In addition, we will discuss the complementarity between the velocity and the length of the filament as they can not be determined simultaneously.

## 1. Introduction

Actin and myosin are well known proteins that cause both muscle contractions and protoplasmic streaming, or cell motility. The *in vitro* motility assay of actin filaments has been utilized since the late 1980s, to help understand the mechanism of actin-myosin interaction (HIGASHI-FUJIME, 1986; KRON and SPUDICH, 1986; HARADA *et al*., 1987; TOYOSHIMA *et al*., 1988; HUXLEY, 1990). In a motility assay, the sliding movements of actin filaments will occur when the actin filaments are mixed with myosin molecules fixed on the surface of a slip cover glass in the presence of ATP. Actin filaments are thin strands with a precise thickness of ~0.01 $\mu$m and variable lengths of about ~10 $\mu$m. This size is much smaller than the resolution of optical microscopes. We can observe the images of actin filaments which are approximately ten times thicker than the actual filaments when they are labeled by fluorescent agents and placed under a fluorescence microscope. Meanwhile, myosin which has a size of approximately ~0.03 $\mu$m in diameter, could not be observed as it was not labeled with the fluorescent agent. In this experiment, the fluorescent image of actin filaments moved in definite directions and altered their forms in a complicated manner.

In past studies of the sliding movements, it has been reported that the average velocity was invariably independent of the length of the actin filament when the temperature and ATP concentration were constant (TAKIGUCH and HIGASHI-FUJIME, 1988; TOYOSHIMA *et al.*, 1988). However, the state of the sliding actin filaments which move in a winding form remains complicated. Therefore it is not easy to accurately determine the velocity of a single filament. In addition, if the transformation of a filament is significant then it is difficult to fully describe the characteristics of the movements.

In this study, we proposed a method to create a "spatiotemporal color pattern" to illustrate characteristics of the sliding movement of a continuous string. In order to examine the capability using color patterns to represent the movements, we at first tested several color patterns that were generated when a line segment with constant length slid unidirectionally. It was shown from the simulation that a pattern could describe the sliding velocity and characteristics such as shifting from a rail like locus, regardless of the complication in the string form. We also processed the actual video images of the fluorescent labeled actin filament sliding in the *in vitro* motility assay into binary thin line images. This was done to digitize the filament images and describe the movement with the spatiotemporal color pattern. Finally, by comparing this pattern with the computer simulated patterns in which the conditions of the sliding velocity and/or locus changed, we can discuss the character of the sliding of the actin filaments. The method to estimate the average velocity from the color pattern, and the possibility of existence of velocity fluctuations and/or of the deviation from the sliding locus are discussed in this paper.

## 2. Method

### *2.1. In vitro motility assay and video fluorescent microscopy*

The video pictures used in this study were taken by Dr. Toshiro ODA who researched the effect of ATP and GTP on the sliding velocity of actin filament. The conditions of in vitro motility assay and the techniques of video fluorescent microscopy have been previously described in detail (ODA *et al.*, 1996).

Actin and myosin were extracted from striated skeletal muscle of a rabbit. The actin filaments were polymerized after the extraction process with acetone-dried powder and then purified according to the method of SUZUKI and MIHASHI (1991) that was a slight modified method of SPUDICH and WATT (1971). These filaments were labeled with phalloidin-tetramethylrhodamine. The extracted myosin was subdivided into 100 $\mu$L of solution and frozen in a small container of plastic micro tubes and stored at –80°C (HARADA *et al.*, 1990). Then myosin heads that are known as HMM (Heavy Mero-Myosin) were refined by $\alpha$-chymotryptic digestion from the stored myosin, following the procedures of OKAMOTO and SEKINE (1985) and KRON *et al.* (1991).

The *in vitro* assay was assembled in the flow cell consisting of a slide glass and a slip glass fixed parallel over two spacers. The inside surface of the flow cell was coated with nitrocellulose. The thin crack of flow cell was filled with a solution. Then myosin was poured in, and that was absorbed by the nitrocellulose (KRON *et al.*,1991). After the excess myosin was removed, fluorescent labeled actin filaments were introduced. Some of the actin filaments combined with the fixed myosin, while others flowed out with the albumin solution. The movement of actin filaments was induced by the addition of the ATP solution.

The solution in the example used for this report was 120 $\mu$M ATP with the presence of 4 mM GTP. The experiment was implemented at a room temperature of 28°C.

The fluorescent images of the sliding actin filaments were caught by a SIT camera (HAMAMATSU C2400-8), and were recorded on video tape at the rate of interlacing one frame per 1/30 second by using the video image control system (HAMAMATSU ARGUS-100). These video images were used for analysis.

### *2.2. Creation of spatiotemporal color patterns*

The images of the sliding movement of actin filament can be assumed as an unidirectional translocation of a transforming line segment. We created the spatiotemporal color pattern in order to illustrate the characteristics of sliding line segments.

We can visualize the movement of line segment utilizing the pattern in which the coordinate values of all the points in the digital line segment are represented by several colors. The method to make color pattern from the coordinate data of line segment is shown in Fig. 1. The color selected to each coordinate value was determined as follows:

$$\begin{cases} C_{Xi}(t) = Xi(t) \mod r \\ C_{Yi}(t) = Yi(t) \mod r \quad (i = 0, 1, \cdots, n-1) \end{cases} \tag{1}$$

where $C_{Xi}(t)$, $C_{Yi}(t)$ are color code numbers of the point $i$ in the line segment at time $t$ for $x$ and $y$ coordinate respectively. $Xi(t)$ and $Yi(t)$ are $x$ and $y$ coordinate values of point $i$ at time $t$. And $r$ is range of the color code. In this study 60 different colors were used (i.e. $r$ = 60). We employed four gradations of red, blue, and green and we excluded four monochrome colors giving us the final 60 colors. These were index colors specified by color code 0 through 59. The colors were placed sequentially along the abscissa from the rear end to the lead tip point of the line segment. And the ordinate is time (as shown in Fig. 1). All points in the line segment were specified by $x$ and $y$ coordinates. Therefore, two color patterns were created for both coordinate values.

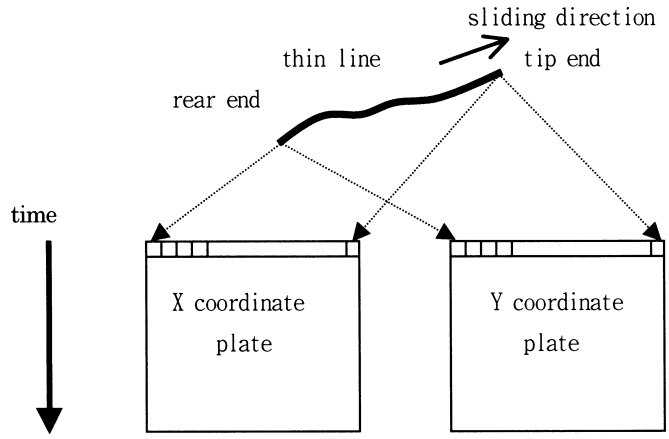


Fig. 1. Method in making a spatiotemporal color pattern.

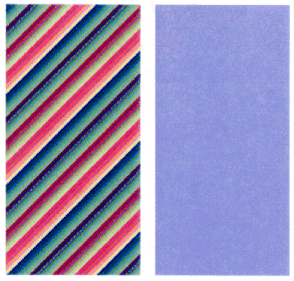

Fig.2 (a)

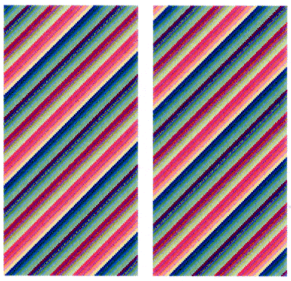

Fig.2 (b)

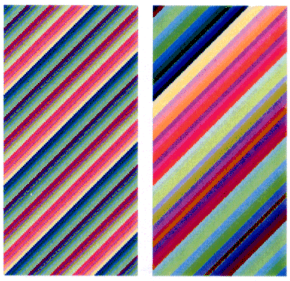

Fig.2 (c)

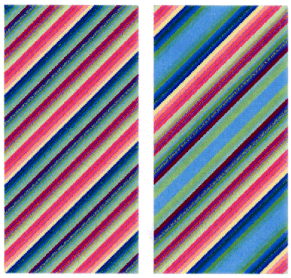

Fig.2 (d)

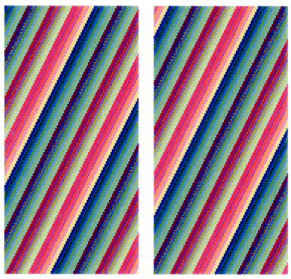

Fig.2 (e)

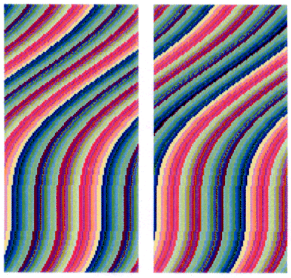

Fig.2 (f)

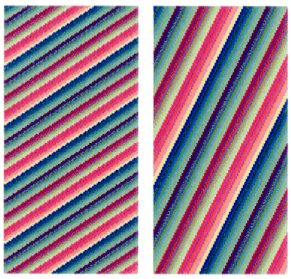

Fig.2 (g)

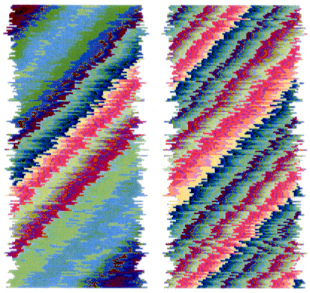

Fig.6

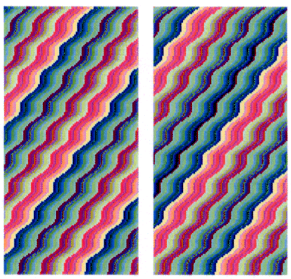

Fig.7 (a)

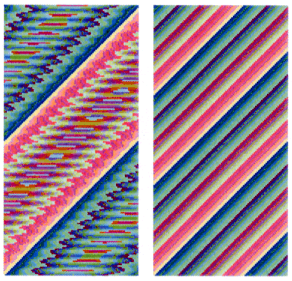

Fig.7 (b)

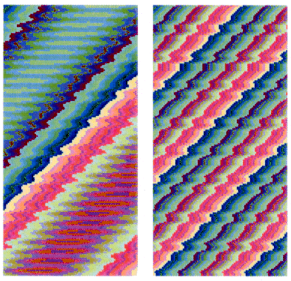

Fig.7 (c)

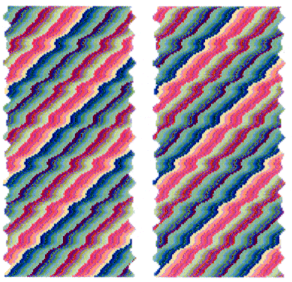

Fig.7 (d)

Fig. 2. Spatiotemporal color pattern of the simulations of the sliding lines (1). (Figures (a)–(g) are printed on the color page.) Color pattern: *X*-plate (left) and *Y*-plate (right). Conditions of the simulations (a)–(g) are shown in the table below:

| Fig. | Line form | Sliding direction (*) | Speed (dot/frame) | Locus |
|---|---|---|---|---|
| (a) | Straight segment | Straight horizontally | 1 | (*a) |
| (b) | Straight segment | Straight 45° (to the lower right) | 1 | (*b) |
| (c) | Straight segment | Straight –15° (to the upper right) | 1 | (*c) |
| (d) | Sine curve | On the sine curve | 1 | (*d) |
| (e) | Straight segment | Straight 45° (to the lower right) | 0.5 | (*e) |
| (f) | Straight segment | Straight –45° (to the upper right) | $1 + \sin(t\,\pi/90)$ | (*f) |
| (g) | Straight segment | Shifts at the side | (1.5, 0.5) | (*g) |

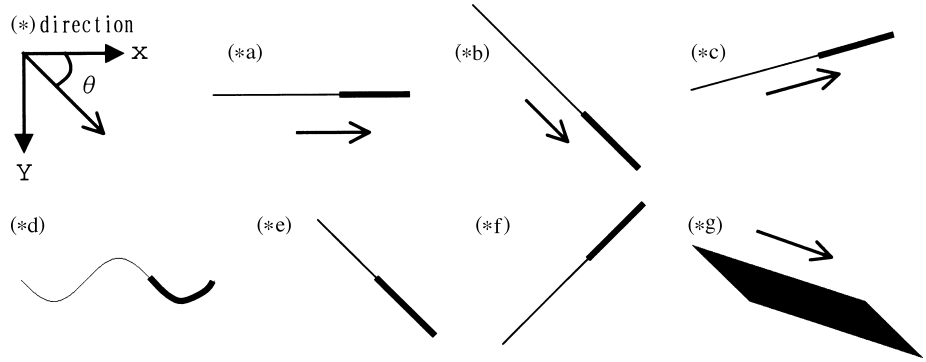


Fig. 6. Spatiotemporal color patterns of the acquired data. (Figure is on the color page.) The left and right patterns are *X* and *Y* coordinate plate respectively. The abscissa in both *X* and *Y* plate were equally ordered from the left to the right according to the spatial filament line from rear end to the front tip. The vertical axis represents the time from top to bottom equaling video frames 2 through 192.

Fig. 7. Spatiotemporal color pattern of the simulations of the sliding lines (2). (Figures are printed on the color page.) Conditions of the simulations (a)–(d) are shown in the table below:

| Fig. | Line form | Characteristic feature | Locus |
|---|---|---|---|
| (a) | Straight segment | Fluctuation in velocity | (*a) |
| (b) | Sine curve | Fluctuation in locus (amplitude vibration) | (*b) |
| (c) | Sine curve | Fluctuation in velocity and locus | (*c) |
| (d) | Straight segment | Fluctuation in the number of dots make up the thinned line | (*d) |

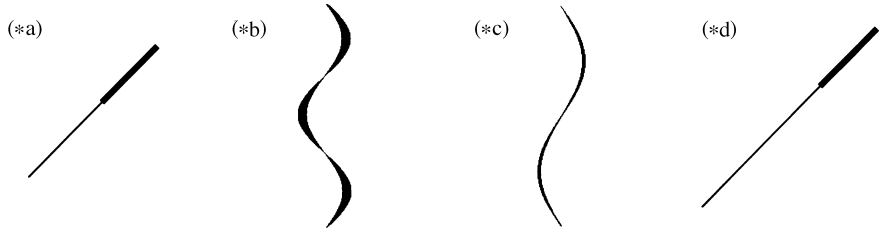

*2.3. Meanings of the slope of the stripes in spatiotemporal color pattern*

In order to comprehend the meaning of the spatiotemporal color patterns, we practiced with several simulations. Our simulation program produced spatiotemporal color patterns by artificially moving the model line segments. All of the model lines in the simulation shown in Figs. 2(a)–(g) had a 90 dot length regardless of their form and they were sliding uniformly at 180 units of time. The generated patterns are shown in Fig. 2. The sliding locus and the conditions of the simulations(a)–(g) are shown in a table in the caption of Fig. 2, respectively. We considered the meaning of the patterns with attention to the relation between sliding conditions such as sliding velocity, locus, and form of the sliding object and slope of stripes appeared in color patterns.

The difference between (a), (b) and (c) (in Fig. 2) was in the directions of their sliding. In these cases straight line segment slid with the uniform velocity of 1 dot per 1 unit of time, and respective directions are 0° (horizontal direction) in the case of (a), 45° in (b) and –15° in (c). The color of the *Y*-plate of simulation(a) was monotone as the straight line segment slid only in an horizontal direction. Except for the *Y*-plate of (a), all the other *X* and *Y* patterns show the same sloping in the stripes.

In the case of (d) the segment form was not straight but a sine curve. It moved as if sliding on a rail (i.e. an sliding object ought to constantly alter its form in accordance to the sliding locus without departing). In this situation the stripes in both the *X* and *Y* pattern also displayed the same slope as the case of straight segment in (a) through (c).

The examples of (e) and (f) were different from the above cases in their sliding velocity. The velocity of (e) was just half of the above cases. The case (f) was specific with the cyclic variable speed made by sine function. The dynamic range of the speed made by the amplitude of the sine function was from 0 to 2 dots per unit of time and the cycle was 180 units of time. It was clearly observed that the slopes of the stripes changed depending on the sliding velocity.

The results of (g) were also distinct from the above cases at the point where the string filament shifted in a side way manner. This type of shifting movement appears in a spatiotemporal pattern as the difference in the slope angle of the stripe between the *x* and *y* coordinate data.

From the above simulations we can say the followings.

(1) The inclination of the stripe pattern in both the *X* and *Y* plates are independent from the sliding directions.

(2) The inclination of the stripe pattern in both the *X* and *Y* plates are independent from the sliding locus or the form of the sliding string object if the form agree with the track of the sliding locus.

(3) The inclination of the stripe pattern depended on the velocity of the sliding.

(4) If the sliding included a shift (a difference between the angle of the object and the direction it moved) then the actual inclinations of the *X* and *Y* plate patterns were different from each other.

With this comprehension we utilized the spatiotemporal color pattern to analyze the characteristics of sliding actin filament captured as the video images.

*2.4. Thinning of filament image by digital image processing*

The equipment employed for the analysis of sliding actin filament was a VHS video

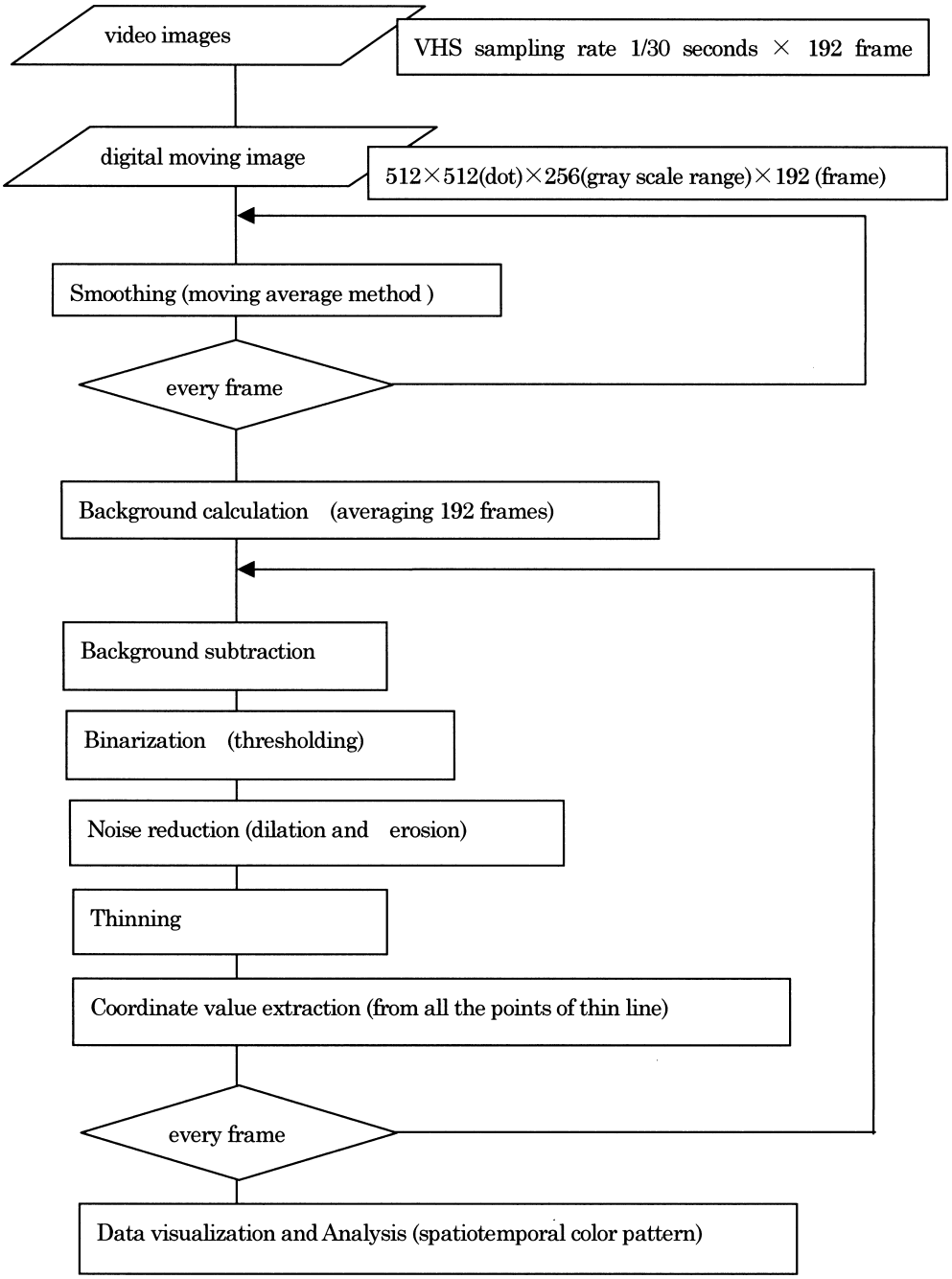


Fig. 3. Flow chart of the image processing.

recorder (Victor VTR HR-S6600) and a personal computer (NEC PC-9821Xn). The picture processing board corresponded to the personal computer (Library Co. LTD. HIMAWARI60 Ver. 1.6) which included the image memory of gray scale 256 range × 512 dot × 512 dot × 192 frame. The programs to process digital images were written in C language (Microsoft C/C++ Ver. 7.0) using the C language function library for HIMAWARI. These were incorporated into the operation software of the HIMAWARI (EASY for MS-DOS) on which digitization from analog images, the continuous display, and general basic image processing depend.

Each video picture reflects a sequence of interlacing monochrome images which were recorded at a rate of one frame for every 1/30 seconds. The digitizing analog video pictures and the digital image sequences were transported directly on line to the computer. By utilizing the digital images as raw object data, these images could be processed into binary thin line images (i.e. medial axes of the images of an actin filament). This was to extract coordinate data and visualize with above mentioned method of the spatiotemporal color pattern. A flow chart of the image processing is shown in Fig. 3.

In this image processing a method of moving average was at first applied to each frame to improve the noisy images. In addition, the brightness in the background of the original picture images was removed. From this point binarization was implemented at the same threshold of each frame. Then almost all noise was reduced by dilating and erosion. After that, the thinning process was applied repeatedly until the binary image of filament became 1 dot width per line. Originally, fluorescence was necessary to observe the actin filaments and could not be seen without it but the fluorescent image appeared thicker than actual actin filament. In this experiment, the scale of the digital images were allotted 94 dots per 10 $\mu$m or approximately 0.1 $\mu$m per dot, and the binary images of filaments has approximately 4–5 dot (0.4–0.5 $\mu$m) width while the width of actual filaments are ~0.01 $\mu$m. Therefore, the thinning process was probably effective or at least harmless even if it would not be precise enough in assisting in the analysis of the characteristics of the sliding movement.

After the thinning process was applied, binary image of the filament with 1 dot width appeared. Also due to the poor condition of the original raw images, that is almost the upper limit of resolution of the apparatus, we had to process the thinned line images with some manual alterations such as repairing broken lines or removing an excess branch of a line. Finally, the sequential images of binary thinned line was obtained and the coordinate values of all points that make up a thinned line were digitized and saved as data file representing each frame.

## 3. Result

### *3.1. Thinned line image and acquired data*

We applied the above mentioned thinning method to the video images of sliding actin filaments. A portion of a long filament and its shape were captured successfully (as shown in Fig. 4(a)). By the algorithm described above (Fig. 3), the raw image data (Fig. 4(a)) was processed into a binary thinned line image (Fig. 4(b)). Then, the $x$ and $y$ coordinate data of integer values was extracted from all the points of the thinned line image and repeated from all frames of the digital images (a part of the data is presented in Table. 1).

The acquired data shown in Table 1 was saved as a computer data file. The movements

of a filament can be reproduced on a computer screen by reading the coordinate data of the lines from the data file and displaying it for each moment (Fig. 5). The thinned lines of the frames 2, 97, and 192 are shown in Fig. 5(a). Figure 5(b) illustrates a sliding locus which was made by superimposing thinned lines from frames 2 through 192. If observed roughly, the filament appears to slide along in a rail-like locus, as the rear portion of the filament traces the track of the front. However, the width of the locus is actually thicker than a 1 dot range which signifies that the rear does not actually follow the front end of the filament (Fig. 5(b)). More details concerning the nature of these sliding movements will be shown with the spatiotemporal color patterns (Fig. 6, see p. 380) below.

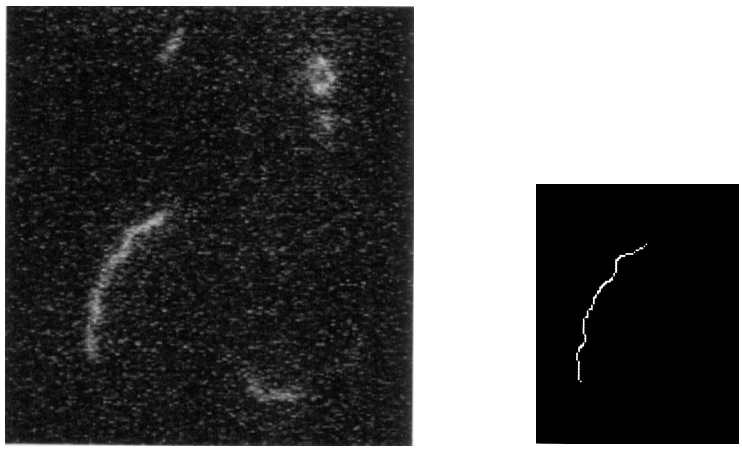

(a) (b)

Fig. 4. Images of actin filaments before and after thinning. (a) The fluorescent image of the actin filament. (b) The thinned line image of the actin filament.

Table 1. The *XY* coordinate values of all the points of the thinned line filament image.

| Frame | N | 0 | 1 | 2 | | 85 | 86 | 87 | 88 | ⋯ | 94 |
|---|---|---|---|---|---|---|---|---|---|---|---|
| 2 | 87 | 75, 8 | 75, 9 | 75, 10 | | 80, 89 | 79, 89 | | | | |
| 3 | 88 | 77, 6 | 77, 7 | 77, 8 | | 80, 87 | 80, 88 | 79, 89 | | | |
| 4 | 89 | 76, 9 | 75, 10 | 75, 11 | | 79, 89 | 78, 89 | 78, 90 | 78, 91 | | |
| ≈⋯ | | | | | | | | | | | |
| 191 | 88 | 28, 160 | 27, 161 | 27, 162 | | 18, 242 | 19, 242 | 20, 243 | | | |
| 192 | 95 | 25, 158 | 26, 159 | 26, 160 | | 17, 238 | 17, 239 | 18, 240 | 18, 241 | ⋯ | 19, 247 |

Frame: Frame number 2-192 (Frame 1 was used for the calculation of the background). Frame interval was 1/30 of a second according to the time series of the video images.

*n*: The number of the points that compose a thin line. Every point was named by a number from the rear of the filament (0) to the lead tip ($n - 1$).

Data: The *X* and *Y* coordinate values of each point of a thin line on the frame image.

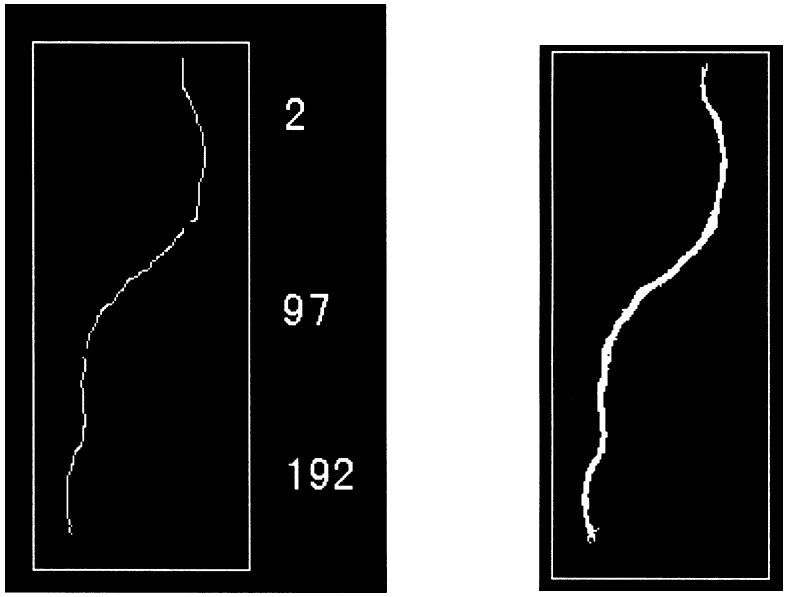


(a) (b)

Fig. 5. The sliding locus of the actin filament. (a) The thinned line of frames 2, 97, and 192. (b) Superimposed frames 2–192 as thinned images.

### *3.2. Data represented by the spatiotemporal color pattern*

We visualized the coordinate values of binary thinned line images of the actual actin filament and their temporal change by the spatiotemporal color pattern according to the method illustrated previously. This color pattern will be utilized from henceforth to consider the characteristics of the sliding filaments as we have described up to this point.

Figure 6 (see p. 380) demonstrates the coordinate values of the points in the thinned line (shown in Table. 1). All the coordinate values of the thinned line image were displayed with 60 different colors by the same method (Fig. 1) as the simulations described before (Fig. 2). The vertical axis (in Fig. 6) represents the time from top to bottom equaling frames 2 through 192. And the abscissa in both $X$ and $Y$ coordinate plate of the pattern were equally ordered from the left to the right according to the filament line from rear end ($i = 0$) to the front tip ($i = n_t - 1$).

Since the number of the points included in the thinned line image of filament ($n_t$) varied in time, we adjusted the horizontal position of each horizontal color bar so that any center points ($i = n_t/2$) were fixed equally on a straight vertical center line at any given time on a spatiotemporal color plate. Possible reasons why the number $n_t$ varied may be the influence of the thinning or other image processing and of the conditions of the original video images or other factors. We assumed the lack of the dots equivalent at the rear end and front end of the thinned line image, and adjusted the position at the center point of the color bars for the present. Further discussion about the fluctuation of $n_t$ will be described

later in Sec. 4.3.

Meanwhile, the pattern in Fig. 6 shows a shifting of stripes from the top of the filament to the rear end as time, and includes high frequency vibrations that make the color patterns appear fuzzy in the plate. The sloping of the stripes on the pattern was measured and it will be described in the next section.

### *3.3. Shifting element and sliding velocity detected from the inclination of the stripes on the pattern*

In this section we will describe the measurement of the inclination of the stripes on the color pattern. In addition, the determination of the sliding velocity and the detection of shifting element in sliding movements are also mentioned with the measurement of the inclination.

The patterns of the data acquired from the thinned line image of actual actin filament shown in Fig. 6 assumed parallel straight lines with regards to the stripes in both $X$ and $Y$ coordinate plates. At first, we measured the inclination of the stripes by fitting parallel straight lines on the patterns and finding the angle of the lines that make dispersion of coordinate data value on the straight lines minimum, changing the line angles by a step of $\pi/80$ radian. As a result, the angle of the line was equal to $\pi/4$ equally in both the $X$ and $Y$ coordinate patterns. This means the sliding velocity was approximately 1 dot per frame.

We also measured the time course of the inclination by calculating the values of

$$\begin{cases} S_X(p,t) = \dfrac{1}{N} \displaystyle\sum_{\substack{0 \le i \le n_t \\ 0 \le i+p \le n_{t-\tau}}} \left\{ X_i(t) - X_{i+p}(t-\tau) \right\}^2 \\ S_Y(p,t) = \dfrac{1}{N} \displaystyle\sum_{\substack{0 \le i \le n_t \\ 0 \le i+p \le n_{t-\tau}}} \left\{ Y_i(t) - Y_{i+p}(t-\tau) \right\}^2 \end{cases} \tag{2.1}$$

and

$$S(p,t) = \frac{1}{2} \left\{ S_X(p,t) + S_Y(p,t) \right\} \tag{2.2}$$

where $Xi(t)$ and $Yi(t)$ are the $x$ and $y$ coordinate value of the point $i$ ($i$ = 0, 1, $\cdots$; $n_t$) at time $t$ on the $X$ and $Y$ plate of the color pattern respectively, and $n_t$ is the number that make up the horizontal color bar at time $t$. $N$ is the number of points that satisfy the inequalities of $0 \le i \le n_t$ and $0 \le i + p \le n_{t-\tau}$, where $\tau$ is the time interval to determine the local inclination. If $\tau$ was small enough so that two horizontal color bars at time $t$ and $t - \tau$ would include a part of the same stripe of the color pattern (i.e. the two thinned lines at time $t$ and $t - \tau$ would overlap each other within the sliding movement), the movement of the stripe between these two color bars were determined by $p$ which made the value $S_X(p)$ or $S_Y(p)$ minimum respectively. We found that $p$ for each time of $t$ ($\ge\tau$) by calculating the value of $S_X(p)$ or $S_Y(p)$ for any $p$. From this point we will note these values of $p$ as $p_X(t)$ and $p_Y(t)$. Also we

found $p(t)$ utilizing the same method to $S(p, t)$ instead of $S_X(p, t)$ or $S_Y(p, t)$. Then we calculated the values of

$$\begin{cases} V_X(t) = \dfrac{p_X(t) + (n_t - n_{t-\tau})/2}{\tau}, \\ V_Y(t) = \dfrac{p_Y(t) + (n_t - n_{t-\tau})/2}{\tau} \end{cases} \tag{3.1}$$

and

$$V(t) = \frac{p(t) + (n_t - n_{t-\tau})/2}{\tau}. \tag{3.2}$$

We assumed the time series of $V_X(t)$ and $V_Y(t)$ as the inclinations of stripes on $X$ or $Y$ plate respectively at time $t$ when horizontal color bars were adjusted at the point of $n_t/2$ as shown in Fig. 6. And $V(t)$ was virtual inclination calculated from least square of the total of $x$ and $y$ coordinate differences (Eq. (2.2)). Moreover we also defined the difference between $V_X(t)$ and $V_Y(t)$ as

$$\delta(t) = V_X(t) - V_Y(t). \tag{4}$$

We used the value of $\delta(t)$ as the index of the shifting element in the sliding movement.

The actual values calculated with the time interval $\tau$=10 were as follows. The average of $V_X(t)$ from $t$ = 12 through 192 was 1.01 dot/frame with the standard deviation of 0.34. On the other hand $V_Y(t)$ was 0.99 ± 0.32 (mean ± std. dev.) dot/frame. And the value of $\delta(t)$ was distributed from –4 to 5 dot/frame with the standard deviation of 1.60 within that observed time. Moreover $V(t)$ was measured 0.99 ± 0.02 (mean ± std. err.) dot/frame.

## 4. Discussion

### *4.1. Characteristics of the sliding*

In order to understand the cause of disorder of the stripes in the color pattern illustrating acquired data (shown in Fig. 6), we continued the simulation that made artificial color pattern again in the same manner described in Sec. 2.3. From the results of the above mentioned simulations (Fig. 2), the sliding velocity determined the inclination of the stripe on the color pattern and if the sliding object shifted out from the locus it caused the difference of the inclination between $X$ and $Y$ coordinate plate of the color pattern.

What condition will cause the disorder of the stripe such as shown in Fig. 6? First, we tried to fluctuate sliding velocity in our simulation (shown in Fig. 7(a), see p. 380). In the case of Fig. 7(a) the frequency of the vibration of the velocity was ten times higher than in the simulation shown in Fig. 2(f), which had a cycle of 180 units of time. The fluctuation of sliding velocity caused vibrations in the slopes of the color pattern. Next, we experimented

with a case of shifting movement. The simulations of Fig. 7(b) were a slightly modified version of Fig. 2(d), which slid on the sine curve as if moving on a complete rail like locus. Figure 7(b) exhibited vibrations in the amplitudes of the sine curve which provoked some shifting out side of the rail. Vibrations of shifting from the locus caused a difference in the stripe between *X* and *Y* and a disordering of the stripe pattern. In the case of Fig. 7(c) both the fluctuation in the sliding velocity and the vibrations in the locus are included in this simulation, which appears more similar to Fig. 6 than any other one of the simulations shown in Figs. 2 and 7.

From the result of these simulations the characteristics of sliding movement may be described as follows. As rough characteristics the sliding velocity was actually uniform and that the locus and shape were on the same rail. But the disorder in the pattern suggests that a more in depth observation of the movements shows some degree of fluctuation in the velocity and sliding locus.

The results from these simulations illustrates that the velocity and locus vibrations copied the disorder in the pattern of the actual sliding shown in Fig. 6, but this does not exclude the possibility of other influences. For example, fluctuation of the length of the sliding object also caused the vibration in the pattern as shown in Fig. 7(d).

### *4.2. Definition of the sliding velocity of a winding filament*

The angles of lines fitted on the stripes in both *X* and *Y* coordinate patterns were equally $\pi/4$ radian as mentioned in Sec. 3.3. This means the sliding velocity was approximately 1 dot per frame. This signifies that the actual sliding movement has an average velocity in movement (during the total 6.3 seconds of observation) of approximately ~3 $\mu$m/s.

In more detailed calculation, to acquire the time series of $V(t)$ determined by Eq. (3.2) (described in Sec. 3.3.), the averaged velocity was measured as $3.17 \pm 0.08$ $\mu$m/s with $\tau$=10. This $V(t)$ also showed a fluctuation from –2.55 to 9.57 $\mu$m/s with the standard deviation of 1.90 seen in a more short time interval of $\tau = 5$ (in Eq. (3.2)). The shifting element $\delta(t)$ (Eq. (4)) was also detected as mentioned above. These results agreed with the considerations from the simulations (Fig. 7) suggesting that the possible reason for the disorder of the stripes in the color pattern was due to a fluctuation in the sliding velocity and/or shifting from the sliding locus.

The method of determining the sliding velocity from the spatiotemporal color pattern was effective in ascertaining the velocity of the strand object as it transformed while sliding unidirectionally. The spatiotemporal color method was superior to usual methods. In the usual methods, typically short actin filaments were selected and then the velocity was calculated from moving distances of the points at the center of mass of the binary filament images, or calculated from the moving positions of the front or the end of the tail by sampling coordinate positions from the video images. If the velocity of the same filament in this study were determined by the conventional method calculating such simple value as

$$v(t) = \frac{\sqrt{\left\{X_{n_t/2}(t) - X_{n_{t-\tau}/2}(t-\tau)\right\}^2 + \left\{Y_{n_t/2}(t) - Y_{n_{t-\tau}/2}(t-\tau)\right\}^2}}{\tau} \tag{5}$$

the value would be measured smaller than in reality, and would strongly depend on the time interval $\tau$ because the straight distance of the center points were shorter than the winding locus and the difference becomes larger with the larger $\tau$. Actually, conventional $v(t)$ (in Eq. (5)) was measured as $3.13 \pm 0.13$ $\mu$m/s ($\tau = 5$) and $2.99 \pm 0.08$ $\mu$m/s ($\tau = 10$) from the same data by which the velocity $V(t)$ (in Eq. (3.2)) was estimated as $3.17 \pm 0.14$ $\mu$m/s ($\tau = 5$) and $3.17 \pm 0.08$ $\mu$m/s ($\tau = 10$) utilizing the new method. Furthermore, the new definition and the method made it possible to measure the velocity of winding long filament.

*4.3. Fluctuations in the number of dots in the thinned lines*

In the acquired data (shown in Table 1. and Fig. 6), the actual number of dots that make up the thinned line of a filament was distributed from 72 to 98 among the 191 frames used in the study. The average was 86 with a standard deviation of 5.2. The fluctuation in the length was not canceled even if one corrects the error with a revision of $2^{1/2}$ becoming a diagonal interval in the lattice points. The corrected values were 92.8 as an average with a standard deviation of 5.0. This could be converted to a length of $9.2 \pm 0.5$ (std. dev.) $\mu$m, and the maximum fluctuation in length became 1.3 $\mu$m. One of the reasons why the number of dots fluctuates is due to negative effects of the image condition and processing. If the brightness of the filament or the background in the raw video picture was different from other frames then the length of the processed line showed variable fluctuations in length.

Assuming these differences to be equivalent at the area around the front and tail end of the filament, we placed the color bar as fixed at the center of the line as shown in Fig. 6. On the other hand, there is no guarantee concerning the equivalency in both end. It was possible that poor conditions such as after imaging were different at the tail end as the front end progressed in direction. Moreover the possibility of actual length change of actin filament has been recently reported (HONDA *et al*., 1999; SHIMO *et al*., 1999) even if the constancy in the length may have been generally supposed for long time. Also, if the number of dots make up the thinned line image of actin ($n_t$) change in a nonequivalent manner between the rear and front end of the filament, then there are no correct reasons as to why the center point of the color bar was adjusted in the spatiotemporal color pattern. In addition, if this kind of data is still fixed at the rear end ($i = 0$) or the front end ($i = n_t$) or the center point ($i = n_t/2$) indiscriminately, the color pattern shows a disorder in the stripe (shown in the simulation of Fig. 7(d)). The influence of the fluctuation of $n_t$ can not be separated from the influence of fluctuation of the velocity. They are alternatives and we can not measure both of them correctly without any assumptions even if utilizing our new method. So, it must be noted that the velocity $V(t)$ (Eq. (3.2)) is determined with the fixed point of the center, while the value of $\delta(t)$ (Eq. (4)) was independent from this problem because that factor was canceled by subtraction. The new method is still more effective than the conventional method in determining the longitudinal velocity regardless of the sliding form or direction.

The actual length change caused by the elasticity of the actin filament may be due to the interaction with myosin or some other factor related to movement such as friction with the solution. As the length of change, or differences in the sliding activity between the front and tail end, were related to the physical flexibility of the actin filament as well as the power transmitting mechanism of myosin during sliding, it opens up other questions to our problem. Answers to these inquires will be addressed in another study.

This study was supported by THE HORI INFORMATION SCIENCE PROMOTION FOUNDATION. We would like to thank Dr. Toshiro ODA for all his suggestions, knowledge and the provision of video images used in this study. We also express our thanks to Dr. Yoshiyuki KITAOKA and Dr. Kenji OOSAWA for their useful discussions and Mr. Paul Lege for his advice on English.

## REFERENCES

HARADA, Y., NOGUCHI, A., KISHINO, A. and YANAGIDA, T. (1987) Sliding movement of single actin filaments on one-headed myosin filaments, *Nature*, **326**, 805–808.

HARADA, Y., SAKURADA, K., AOKI, T., THOMAS, D. D. and YANAGIDA, T. (1990) Mechanochemical coupling in actomyosin energy transduction studied by in vitro movement assay, *J. Mol. Biol.*, **216**, 49–68.

HIGASHI-FUJIME, S. (1986) In vitro movements of actin and myosin filaments from muscle, *Cell Motil. Cytoskeleton*, **6**, 159–162.

HONDA, H., HATORI, K., IGARASHI, Y., SHIMADA, K. and MATSUNO, K. (1999) Contractile and protractile coordination within an actin filament sliding on myosin molecules, *Biophys. Chem.*, **80**, 139–143.

HUXLAY, H. E. (1990) Sliding filaments and molecular motile systems, *J. Biol. Chem.*, **265**, 8347–8350.

KRON, S. J. and SPUDICH, J. A. (1986) Fluorescent actin filaments move on myosin fixed to a glass surface, *Proc. Natl. Acad. Sci. USA*, **83**, 6272–6278.

KRON, S. J., TOYOSHIMA, Y. Y., UYEDA, T. Q. P. and SPUDICH, J. A. (1991) Assays for actin sliding movement over myosin-coated surfaces, *Method Enzymol.*, **196**, 399–416.

ODA, T., SHIKATA, Y. and MIHASHI, K. (1996) Mutual sensitization of ATP and GTP in driving F-actin on the surface-fixed H-meromyosin, *Biophys. Chem.*, **61**, 63–72.

OKAMOTO, Y. and SEKINE, T. (1985) A streamlined method of subfragment one preparation from myosin, *J. Biochem.*, **98**, 1143–1145.

SHIMO, R., HASEGAWA, S. and MIHASHI, K. (1999) Fluctuation in the Length of Actin Filament Specific to the Sliding Movement, The 7th JST International Symposium—Molecular Process and Biosystems, 2-3-8, Feb 24, 1999, Tokyo, Japan (Poster session).

SPUDICH, J. A. and WATT, S. (1971) The regulation of rabbit skeletal muscle contraction. I. Biochemical studies of the tropomyosin-troponin complex with actin and the proteolytic fragments of myosin, *J. Biol. Chem.*, **246**, 4866–4871.

SUZUKI, N. and MIHASHI, K. (1991) Binding mode of cytochalasin B to F-actin is altered by lateral binding of regulatory proteins, *J. Biochem.*, **109**, 19–23.

TAKIGUCHI, K. and HIGASHI-FUJIME, S. (1988) In vitro sliding movement of F-actin with HMM and S-1, *Cell Motil. Cytoskeleton*, **10**, 347.

TOYOSHIMA, Y. Y., KRON, S. J. and SPUDICH, J. A. (1988) Observation of in vitro movement of actin filaments directed by myosin fragments bound to a nitrocellulose surface, *Cell Motil. Cytoskeleton*, **10**, 347.